

## Gamma Ray Transitions following keV Neutron Capture in 2s-1d Shell Nuclei

M. J. Kenny,<sup>A</sup> P. W. Martin,<sup>B</sup> L. E. Carlson<sup>C</sup> and J. A. Biggerstaff<sup>D</sup>

<sup>A</sup> AAEC Research Establishment, Private Mail Bag, Sutherland, N.S.W. 2232.

<sup>B</sup> University of British Columbia, Vancouver, Canada, and AAEC Research Establishment.

<sup>C</sup> AINSE Fellow at the Australian National University, and attached to AAEC.

<sup>D</sup> Oak Ridge National Laboratory, Tennessee, U.S.A., and AAEC Research Establishment.

### Abstract

A Ge(Li) detector has been used to observe  $\gamma$ -ray transitions after the capture of keV neutrons in natural samples of F, Al, Si, S and Ar. Transitions to positive and negative parity states show that there are strong p-wave resonances as well as s-wave resonances in this mass region. The even- $Z$  nuclei decay more by E1 transitions than by M1. Odd- $Z$  nuclei decay by strong M1 transitions.

### Introduction

Previous measurements of keV capture spectra for elements in the  $A = 20-40$  region have used NaI detectors (Bird *et al.* 1965; Bergqvist *et al.* 1967; Lundberg and Bergqvist 1970; Nystrom *et al.* 1970). From these experiments a certain amount of information has been derived for electric and magnetic dipole transitions following p-wave and s-wave resonance capture. In this laboratory, techniques have been developed for using Ge(Li) detectors for resolved resonance capture (Bird *et al.* 1968). In the region  $A = 40-70$  strong s-wave resonances are seen and there is evidence for d-wave resonances (Bird *et al.* 1969) consistent with shell model theory. An extension of this work to cover six elements between  $A = 90$  and 140 has shown strong dipole transitions following p-wave capture, again consistent with shell model theory (Bird *et al.* 1972). Detailed analysis of this work is hindered by the close spacing of both initial and final states.

It was decided to seek further clarification of the significance of p-wave resonances with mass number and of the contributions of electric and magnetic radiation in the decay schemes by using a high resolution Ge(Li) detector to study keV capture by several 2s-1d shell nuclei. The samples used were fluorine, aluminium, silicon, sulphur and argon.

### Method

The experimental techniques have been described previously (Bird *et al.* 1969). The detector used for these measurements was an Ortec 40 cm<sup>3</sup> coaxial Ge(Li), with a resolution (FWHM) of 2.3 keV at 1.33 MeV. The detector was at 90° to the capture sample. Neutrons were produced with the  ${}^7\text{Li}(p,n){}^7\text{Be}$  reaction using a proton energy 12 keV above threshold and a thick target. The proton beam was klystron bunched to 2 ns FWHM and the timing resolution was  $< 4$  ns for the  $\gamma$ -ray energy range from 700 keV to 9 MeV. The flight path length to sample centre was 30 cm. Digital window techniques were used in the time spectrum to select

four or five intervals of neutron energy. The neutron energy was also measured to an accuracy of  $\pm 4$  keV by the shift in energy of primary  $\gamma$ -rays above the expected thermal value.

Table 1. 2s-1d shell nuclei resonance parameters

Nucleus	Resonance energy (keV)	Reference	$I_n$	$J^\pi$	Observed in present work
$^{19}\text{F}$	27.07	Macklin and Winters (1973)	1	$2^-$	Yes
	49.7	Macklin and Winters (1973)	1	$1^-$	Yes
$^{27}\text{Al}$	6	Bergqvist <i>et al.</i> (1967)	1	—	No
	34.7	Singh <i>et al.</i> (1971)	0	$2^+$	Yes
$^{28}\text{Si}$	32–38 <sup>A</sup>	Bergqvist <i>et al.</i> (1967)	—	—	Yes
	67.7	Allen and Macklin (1973)	—	—	Yes
$^{32}\text{S}$	30	Bergqvist <i>et al.</i> (1967)	1	$3/2^-$	Yes
	43	Nystrom <i>et al.</i> (1970)	—	—	Yes

<sup>A</sup> Two or more resonances.

Gamma ray energy calibration was made in terms of the  $^1\text{H}(n, \gamma)^2\text{H}$  line at 2223 keV, the thorium line at 2614 keV and iron and titanium thermal capture lines at 7646 and 6413 keV (Rasmussen *et al.* 1970; Gove and Wapstra 1972). Detector efficiency measurements were performed with a  $^{56}\text{Co}$  source and the reactions  $^{26}\text{Mg}(p, \gamma)^{27}\text{Al}$ ,  $^{14}\text{N}(n, \gamma)^{15}\text{N}$  and  $^{35}\text{Cl}(n, \gamma)^{36}\text{Cl}$  (Bartholomew *et al.* 1967; Fubini *et al.* 1970). Data were collected by an on-line PDP7 computer. Pure element samples were used for aluminium, silicon, sulphur and argon while Teflon was used for a fluorine sample. Sample masses were typically 2 kg and run times varied from 40 to 80 h with an average beam current of 6  $\mu\text{A}$ . Measured intensities varied from a few thousand counts in the strongest peaks to about fifty counts in the weakest peaks. Uncertainties on measured intensities due to statistical errors, background, efficiency corrections and variation in self-absorption thus vary from a few per cent for the strongest transitions up to about 30% for the weakest.

## Results

A list of resonances for which  $\gamma$ -ray spectra have been measured is given in Table 1. The observed transitions and relative intensities (per 100 captures) are listed in Tables 2a–2f together with thermal capture and previous keV data where available. Decay schemes and high energy  $\gamma$ -ray spectra are shown in Figs 1–5. The results are generally consistent with previous work, but remove numerous ambiguities associated with relatively poor resolution NaI experiments.

There are some differences between our results and those of Lundberg and Bergqvist (1970). For the 67.7 keV resonance in  $^{28}\text{Si}$  we observe no measurable intensity to the 3067 keV  $5/2^+$  state whereas they see this as a moderate transition. For the 30 keV resonance in  $^{32}\text{S}$  we observe an increased intensity to the 3221 keV  $3/2^-$  state and negligible intensity to the 2869 keV  $(3/2, 5/2)^+$  state. It must be presumed that because of the superior resolution of the Ge(Li) detector, the present decay scheme is the more reliable.

Radiation widths have been calculated from the usual formulae (Skorka *et al.* 1966) and are listed in Table 3. In cases of uncertainty, both E1 and M1 radiation widths are included. Higher multiplicities have not been calculated because they are unusual in neutron capture.

Large M1 radiation widths are partly due to the preferred 8.3 eV value for  $\Gamma_\gamma$  in aluminium taken from the data of Singh *et al.* (1971). From the 49 observed transitions, 25 are E1, 20 are M1 and 4 are uncertain. The 38 keV resonance in silicon and the 43 keV resonance in sulphur have equal numbers of E1 and M1 transitions irrespective of  $l = 0$  or 1 assignment. Average radiation widths are  $3.3 \times 10^{-3}$  W.u. for E1 and  $90 \times 10^{-3}$  W.u. for M1. Interchanging the uncertain E1 and M1 transitions has a negligible effect on the average. Similarly, any error caused by assuming  $\Gamma_\gamma = 1.0$  eV in the unknown cases has negligible effect.

Table 2. Gamma rays observed after keV neutron capture

References to data compared with the present results are:

Bq, Bergqvist *et al.* (1967);

Bt, Bartholomew *et al.* (1967);

Hd, Hardell and Hasselgren (1969), Hardell *et al.* (1969);

Lb, Lundberg and Bergqvist (1970);

Sp, Spilling *et al.* (1968);

St, Spits *et al.* (1970)

(a) Resonances in  $^{19}\text{F}$

$\gamma$ -ray energy <sup>A</sup> (keV)	Transition ( $^{20}\text{F}$ state) (keV)	$J_\pi^\pi$	Thermal <sup>B</sup> Sp, Hd	Intensity/100 captures		44 keV Present	49 keV	
				27 keV Present	Bq		Bq	Present
6601	$R \rightarrow 0$	$2^+$	9.0	$2.0 \pm 0.5$			5	
5955	$R \rightarrow 656$	$3^+$		$6 \pm 1$	6	$42 \pm 7$	9	
5778	$R \rightarrow 823$	$4^+$				$23 \pm 7$		
5617	$R \rightarrow 984$	$1^-$	1.2				13	$18 \pm 4$
5544	$R \rightarrow 1057$	$1^+$	4.4				12	$9 \pm 4$
5290	$R \rightarrow 1309$	$2^-$	1.8	$31 \pm 2$	32			
4757	$R \rightarrow 1843$	$(2)^-$	1.4	$8 \pm 2$				
4630	$R \rightarrow 1971$	$(3)^-$	0.1	$46 \pm 4$	50			
4556	$R \rightarrow 2044$	$2^+$	4.7	$1.5 \pm 1$			42	$59 \pm 6$
3635	$R \rightarrow 2966$	$2^+, 3^+$				$35 \pm 9$		
3112	$R \rightarrow 3488$	$1^+$	2.0	$3 \pm 1$	8		20	$14 \pm 5$
2518	$R \rightarrow 4082$	$1^+$	0.5	$2.5 \pm 1$	5		7	
Secondaries								
823	$823 \rightarrow 0$		2.0			$45 \pm 7$		
851	$1843 \rightarrow 984$			$2.5 \pm 1$				
985	$984 \rightarrow 0$		9.3	$4 \pm 1$				$17 \pm 4$
1057	$1057 \rightarrow 0$		6.2	$2.5 \pm 1$				$14 \pm 6$
1147	$1971 \rightarrow 823$		2.3	$24 \pm 3$				
1307	$1309 \rightarrow 0$		4.4	$48 \pm 4$				
1386	$2044 \rightarrow 656$		6.6	$5 \pm 1$				$57 \pm 6$
1841	$1843 \rightarrow 0$		6.5	$8 \pm 2$				
1892	$4082 \rightarrow 2195$		0.5	$1.5 \pm 0.5$				
1970	$1971 \rightarrow 0$		0.8	$9 \pm 2$				
2143	$2966 \rightarrow 823$		2.0			$18 \pm 4$		
2195	$2195 \rightarrow 0$		0.7	$1.5 \pm 0.5$				
2966	$2966 \rightarrow 0$		0.9			$11 \pm 3$		
3490	$3488 \rightarrow 0$		6.7	$2.5 \pm 1$				$14 \pm 5$
4080	$4082 \rightarrow 0$		0.4	$1.5 \pm 0.5$				

<sup>A</sup>  $E_\gamma(\text{measured}) - E_n$ .

<sup>B</sup> Only those lines seen in keV capture are included here.

Table 2 (Continued)  
(b) Resonance in <sup>27</sup>Al

$\gamma$ -ray energy <sup>A</sup> (keV)	Transition ( <sup>28</sup> Al state) (keV)	$J^{\pi}_I$	Thermal Hd	Intensity/100 captures		Bq
				35 keV Present		
7724	$R \rightarrow 0$	$3^+$	31.8	$79 \pm 5$		60
7689	$R \rightarrow 31$	$2^+$	4.5	$2.5 \pm 1$		4
6708	$R \rightarrow 1014$	$(3)^+$	1.0	$3 \pm 1$		
6102	$R \rightarrow \begin{smallmatrix} 1620 \\ 1623 \end{smallmatrix}$	$\begin{smallmatrix} 1^+ \\ (2,3)^+ \end{smallmatrix}$	2.9	$10 \pm 2$		10
5579	$R \rightarrow 2139$	$(2,3)^+$	1.1	$1.5 \pm 1$	}	4
5445	$R \rightarrow 2272$		0.2	$2 \pm 1$		
2956	$R \rightarrow 4766$	$(I = 1)$	9.3	$2 \pm 1$		
2818	$R \rightarrow 4905$	$(I = 1)$	3.5			3
Secondaries						
1623	$\begin{smallmatrix} 1620 \\ 1623 \end{smallmatrix} \rightarrow 0$		2.3	$6 \pm 1.5$		
1017	$1017 \rightarrow 0$		2.8	$2.0 \pm 1$		
986	$1017 \rightarrow 31$		2.3	$2.5 \pm 1$		
868	$3011 \rightarrow 2143$			$3.5 \pm 1$		

(c) Resonances in <sup>28</sup>Si

$\gamma$ -ray energy <sup>A</sup> (keV)	Transition ( <sup>29</sup> Si state) (keV)	$J^{\pi}_I$	Thermal St	Intensity/100 captures		Lb
				38 keV Present	67.7 keV Present	
8476	$R \rightarrow 0$	$1/2^+$	2.4	$9 \pm 1.5$	$32 \pm 2$	35
7202	$R \rightarrow 1273$	$3/2^+$	8	$47 \pm 3$	$37 \pm 2$	32
6449	$R \rightarrow 2028$	$5/2^+$	0		$19 \pm 2$	10
6049	$R \rightarrow 2426$	$3/2^+$	0.5		$9 \pm 1$	8
	$R \rightarrow 3067$	$5/2^+$				7
3540	$R \rightarrow 4934$	$3/2^-$	69	$42 \pm 3$	$2 \pm 1$	9
2092	$R \rightarrow 6381$	$1/2^-$	21	$2 \pm 1$	$1.0 \pm 0.5$	(17)
Secondaries						
2027	$2028 \rightarrow 0$			$15 \pm 2$	$5 \pm 1$	
4935	$4934 \rightarrow 0$		65	$56 \pm 2$	$6 \pm 1$	
6383	$6381 \rightarrow 0$		12	$15 \pm 2$	$4 \pm 1$	

(d) Resonances in <sup>29</sup>Si

$\gamma$ -ray energy <sup>A</sup> (keV)	Transition ( <sup>30</sup> Si state) (keV)	$J^{\pi}_I$	Thermal St	Intensity/100 captures	
				15 keV Present	26 keV Present
10612	$R \rightarrow 0$	$0^+$	20	$80 \pm 10$	0
8380	$R \rightarrow 2232$	$2^+$	5	$20 \pm 10$	100

<sup>A</sup>  $E_{\gamma}(\text{measured}) - E_n$ .

**Table 2 (Continued)**  
(e) Resonances in  $^{32}\text{S}$

$\gamma$ -ray energy <sup>A</sup> (keV)	Transition ( $^{32}\text{S}$ state) (keV)	$J_f^\pi$	Intensity/100 captures				
			Thermal	30 keV		43 keV	
				Present	Lb	Present	Lb
8640	$R \rightarrow 0$	$3/2^+$	2.5	$5 \pm 1.5$	3	$8 \pm 2$	17
7799	$R \rightarrow 842$	$1/2^+$	3.5	$48 \pm 3$	50	$6 \pm 2$	(10)
6671	$R \rightarrow 1968$	$5/2^+$		$4 \pm 1$	10		(5)
6325	$R \rightarrow 2313$	$3/2^+$		$4 \pm 1$	10	$9 \pm 2$	
	$R \rightarrow 2869$	$\begin{pmatrix} 3/2^+ \\ 5/2^+ \end{pmatrix}$			4		
5415	$R \rightarrow 3221$	$3/2^-$	52.6	$27 \pm 3$	8	$60 \pm 4$	66
4424	$R \rightarrow 4213$	$3/2^-$	4.3	$6 \pm 1.5$	4	$9 \pm 2$	
2929	$R \rightarrow 5715$	$1/2^-$	14.0	$5 \pm 1.5$	15	$8 \pm 2$	(7)
Secondaries							
5042	$5883 \rightarrow 842$			0.6		$0.5 \pm 0.5$	
4862	$5715 \rightarrow 842$			$5 \pm 1$		$6 \pm 1$	
3363	$4213 \rightarrow 842$			$2.5 \pm 1$		$5 \pm 1$	
3218	$3221 \rightarrow 0$			$15 \pm 1$		$31 \pm 3$	
2371	$3221 \rightarrow 842$			$15 \pm 1$		$29 \pm 3$	
2310	$2313 \rightarrow 0$			$2 \pm 1$		$5 \pm 1$	
1968	$1968 \rightarrow 0$			$4 \pm 1$		0	
1698	$4920 \rightarrow 3218$			$2 \pm 1$		2	
1474	$2313 \rightarrow 842$			$4 \pm 1$		8	

(f) Resonances in  $^{40}\text{Ar}$

$\gamma$ -ray energy <sup>A</sup> (keV)	Transition ( $^{40}\text{Ar}$ state) (keV)	$J_f^\pi$	Thermal Bt	Intensity/100 captures	
				15–70 keV Present	58 keV Present
6098	$R \rightarrow 0$	$7/2^-$		$15 \pm 2$	$40 \pm 4$
5933	$R \rightarrow 167$	$5/2^-$		$2.5 \pm 1$	
5582	$R \rightarrow 516$	$3/2^-$	14.6	$1.0 \pm 1$	
5063	$R \rightarrow 1035$		0.8	$10 \pm 2$	$26 \pm 3$
4744	$R \rightarrow 1354$	$3/2^-$	57.6	$71 \pm 3$	$34 \pm 3$
Secondaries					
1187	$1354 \rightarrow 167$			$33 \pm 3$	
838	$1354 \rightarrow 516$			$5 \pm 1$	

<sup>A</sup>  $E_\gamma(\text{measured}) - E_n$ .

### Spin and Parity Assignments

Where the  $l$  value for the resonance is known, the dominant decay mode is dipole, either electric or magnetic. Similar behaviour is observed in keV capture in the regions  $A = 40$ –70 and 90–130, and also occurs across the periodic table in thermal capture. Assuming a preference for dipole transitions and using previously determined spin and parity assignments, a number of deductions can be made.

Table 3. Estimated radiation widths

Neutron resonance	$E_\gamma$ (keV)	$I_\gamma$ ( $\times 10^{-2}$ )	$\Gamma_\gamma$ (eV)	Dipole strength ( $10^{-3}$ W.u.)	
				E1	M1
<i><math>^{19}\text{F}</math> target</i>					
27 keV, $J_\pi^\pi = 2^-$ , p wave	6628	2	1.4 <sup>A</sup>	0.2	
	5982	6		0.75	
	5317	31			140
	4784	8			47
	4657	46			304
	4583	1.5		0.4	
	3139	3		2.7	
	2545	2.5		4.3	
44 keV	5999	42	1.0 <sup>B</sup>	4.0	94
	5822	23		4.4	57
	3679	35		17.0	350
49 keV, $J_\pi^\pi = 1^-$ , p wave	5666	18	1.7 <sup>A</sup>		87
	5593	9		1.7	
	4606	59		20	
	3162	14		15	
<i><math>^{27}\text{Al}</math> target</i>					
35 keV, $J_\pi^\pi = 2^+$ , p wave	7758	79	8.3 <sup>C</sup>		680
	7728	2.5			23
	6743	3			4
	6132	10			174
	5616	1.5			46
	5480	2			58
	2991	2		10	
<i><math>^{28}\text{Si}</math> target</i>					
38 keV	8513	9	0.23 <sup>D</sup>	0.05	2
	7239	47		0.5	14
	3574	42		3.3	100
	2126	2		0.7	21
67.7 keV, deduced p wave	8542	32	0.8 <sup>E</sup>	0.7	
	7268	37		1.2	
	6516	19		0.9	
	6116	9		0.5	
	3603	2			16
	2159	1			38
<i><math>^{29}\text{Si}</math> target</i>					
(32) keV	8406	100	1.0 <sup>B</sup>	2.6	81
<i><math>^{32}\text{S}</math> target</i>					
30 keV, $J_\pi^\pi = 3/2^-$ , p wave	8670	5	0.5 <sup>F</sup>	0.06	
	7829	48		0.7	
	6701	4		0.1	
	6355	4		0.1	
	5445	27			40
	4454	6			16
	2959	5			47

<sup>A</sup> Macklin and Winters (1973).

<sup>B</sup> Presumed value.

<sup>C</sup> Singh *et al.* (1971).

<sup>D</sup> Allen and Macklin (1973);  $g = 1$ .

<sup>E</sup> Allen and Macklin (1973);  $g = 2$ .

<sup>F</sup> Bergqvist *et al.* (1967).

Table 3 (Continued)

Neutron resonance	$E_\gamma$ (keV)	$I_\gamma$ ( $\times 10^{-2}$ )	$\Gamma_\gamma$ (eV)	Dipole strength ( $10^{-3}$ W.u.)	
				E1	M1
<i><math>^{32}\text{S}</math> target</i>					
43 keV	8683	8	$1.0^B$	0.2	6
	7842	6		0.2	6
	6368	9		0.5	17
	5458	60		5.4	178
	4467	9		1.5	49
	2972	8		4.4	148
<i><math>^{40}\text{Ar}</math> target</i>					
58 keV	6150	40	$1.0^B$	2.2	
	5113	26		2.4	
	4794	34		3.9	

<sup>B</sup> Presumed value.

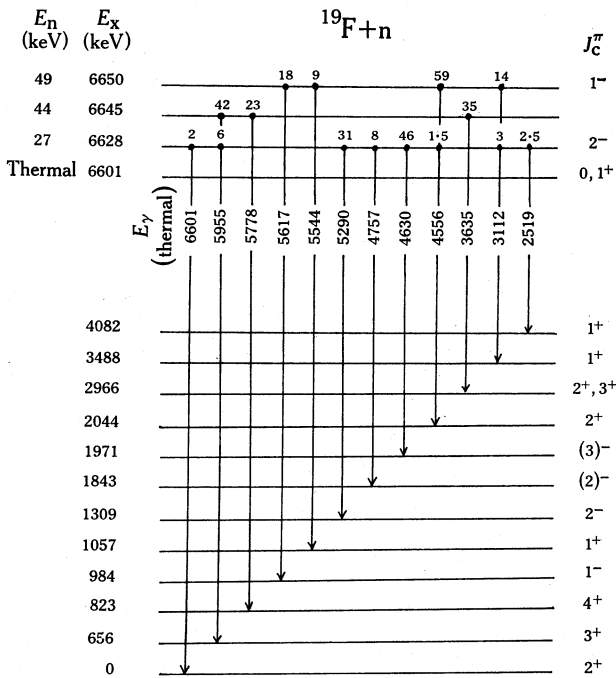


Fig. 1. Decay scheme of  $^{20}\text{F}$  for the 27, 44 and 49 keV resonances in  $^{19}\text{F}$ .

$^{20}\text{F}$ ,  $E_x = 1971 \text{ keV}$ ,  $J_c^\pi = 3^-$

Recent measurements by Longo *et al.* (1973) and Forster *et al.* (1973) assign negative parity to both the 1309 and 1971 keV levels in  $^{20}\text{F}$ . It is probable (Pronko 1973) that the 1971 keV level is the  $3^-$  member of the low lying negative parity quartet ( $1^-, 2^-, 2^-, 3^-$ ) predicted by Johnston *et al.* (1971), the other members being the 984, 1309 and 1843 keV levels. The  $3^-$  assignment is consistent with the strong branch to the  $4^+$  level at 823 keV observed for the 27 keV resonance. Using this  $3^-$  assignment the strongest transitions from this resonance are seen to be M1.

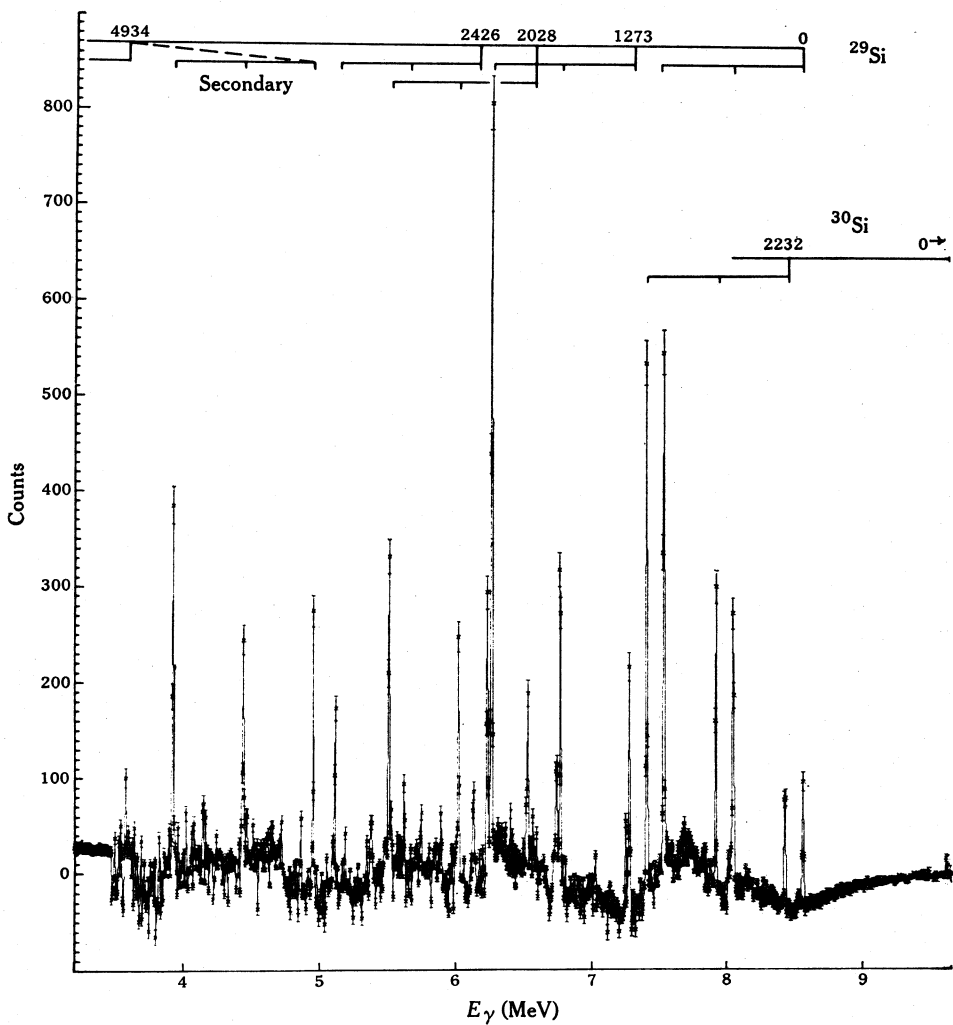


Fig. 2 (above). High energy  $\gamma$ -rays observed in the decay of  $^{29}\text{Si}$  and  $^{30}\text{Si}$ , summed over the neutron energy range 15–70 keV with the continuum subtracted. The positions of full energy, single escape and double escape peaks are shown.

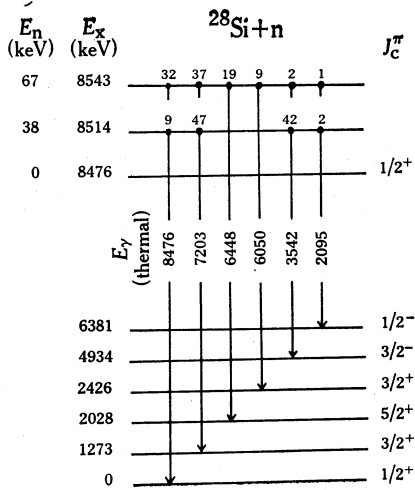


Fig. 3 (left). Decay scheme of  $^{29}\text{Si}$  for the 38 and 67 keV resonances in  $^{28}\text{Si}$ .



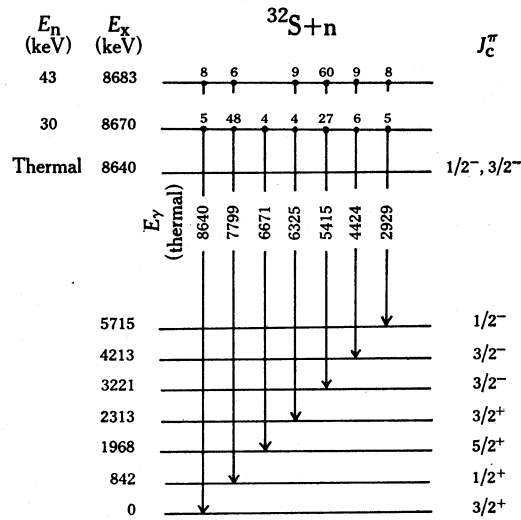


Fig. 4. Decay scheme of  $^{33}\text{S}$  for the 30 and 43 keV resonances in  $^{32}\text{S}$ .

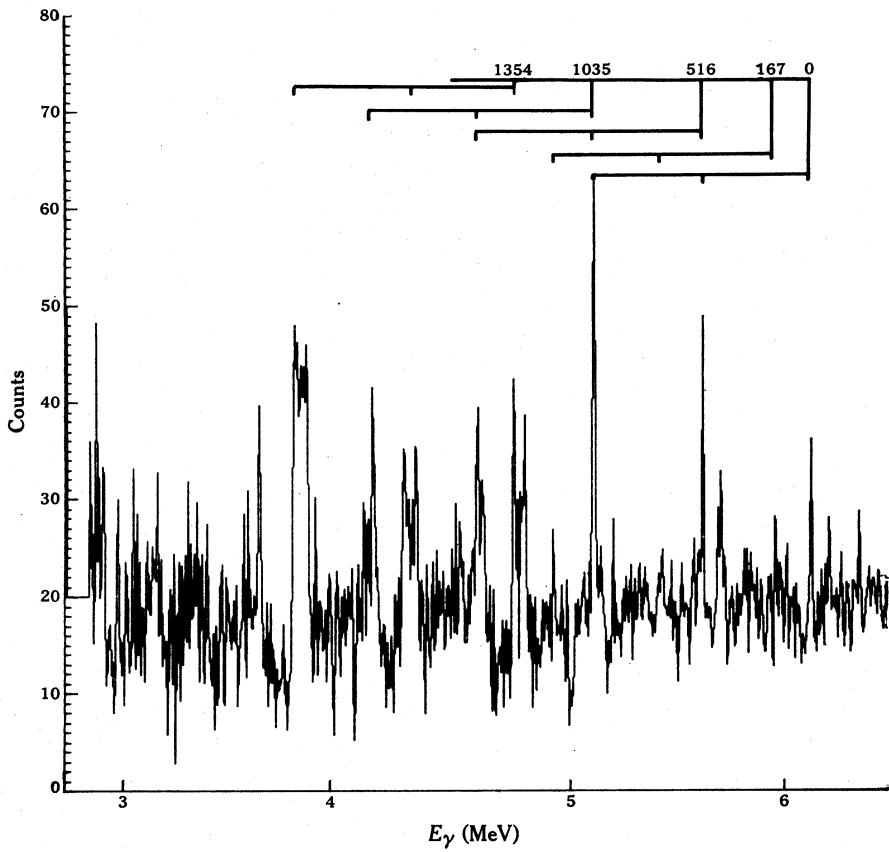


Fig. 5. High energy  $\gamma$ -rays observed in the decay of  $^{41}\text{Ar}$ , summed over the neutron energy range 15–70 keV with the continuum subtracted. The positions of full energy, single escape and double escape peaks are shown.

$^{19}\text{F}+n, E_n = 43.5 \text{ keV} (J_c = 3, 4)$

Two groups of  $\gamma$ -rays are observed here, in agreement with the results of Macklin and Winters (1973), who reported resonances in the capture cross section at  $43.5 \pm 0.1 \text{ keV}$  ( $J_c^\pi \geq 1$ ) and  $48.7 \pm 0.3 \text{ keV}$  ( $J_c^\pi = 1^-$ ,  $\Gamma_n = 1.96 \pm 0.3 \text{ keV}$ ,  $\Gamma_\gamma = 1.7 \pm 0.4 \text{ eV}$ ). Transitions to the levels at 656, 823 and 2966 keV give an observed neutron energy of  $41 \pm 3 \text{ keV}$  and are thus attributed to the 43.5 keV resonance. Because the final states have spins  $(2-4)^+$ , assuming dipole transitions the 43.5 keV resonance then has  $J_c = 3, 4$ .

Table 4. Neutron resonance parameters in natural silicon  
Data from Allen and Macklin (1973)

Resonance $E_n$ (keV)	Area (barn eV)	Width $\Gamma_n$ (eV)	$g \Gamma_n \Gamma_\gamma / \Gamma$ (eV)
31.7	6.5		0.05
38.8	26.3	85	0.23
55.6	36	990	0.45
67.7	106		1.6
70.8	1.9		0.03

$^{28}\text{Si}+n, E_n = 67.7 \text{ keV} (J_c^\pi = 3/2^-)$

High resolution time of flight spectra obtained at ORELA by Allen and Macklin (1973) using a 40 m flight path show five resonances in natural silicon for neutron energies between 20 and 80 keV. The parameters reported for these resonances are given in Table 4. It is seen that the 55 keV resonance is broad and the 67.7 keV resonance is narrow. At a neutron energy of  $(63 \pm 4) \text{ keV}$ , most observed transitions are to positive parity states ( $1/2^+$ ,  $3/2^+$ ,  $5/2^+$ ). The dipole-transition assumption leads to  $J_c^\pi = 3/2^-$  for the 67.7 keV resonance.

A strong similarity is noted between this resonance and the 84 keV p-wave resonance in the neighbouring even- $Z$  nucleus  $^{24}\text{Mg}$ . The latter resonance has  $J_c^\pi = 3/2^-$  and its decay scheme has been reported by Bergqvist *et al.* (1967) and Lundberg and Bergqvist (1970). Almost all the observed transitions are E1 to states with  $J_f^\pi = 1/2^+$ ,  $3/2^+$  and  $5/2^+$ . As is the case with silicon, the decay scheme differs totally from thermal capture, where the strongest transitions are E1 to negative parity states at 3–5 MeV excitation.

$^{29}\text{Si}+n, E_n = (26 \pm 5) \text{ keV} (J_c^\pi = 2^-, l_n = 1)$

Although natural silicon contains only 4.7%  $^{29}\text{Si}$ , the spectra show a strong transition to the  $2^+$  first excited state in  $^{30}\text{Si}$  at  $E_n = (26 \pm 5) \text{ keV}$ . This transition is almost as strong as any observed in  $^{29}\text{Si}$  and, when isotopic abundances are considered, it is about 15 times stronger than any other observed transition. This behaviour is completely different from that for thermal capture (Spits *et al.* 1970). An explanation for the appearance of this transition and the non-appearance of transitions to the  $0^+$  ground state is to assign  $J_c^\pi = 2^-$ . The possibility of the resonance being s wave and the transition being M1 is less likely because of the relatively fewer strong M1 transitions observed in even- $Z$  nuclei than in odd- $Z$  nuclei. The data in Table 4 show that the 31.7 keV resonance in natural silicon has  $g \Gamma_\gamma \Gamma_n / \Gamma \sim 0.05 \text{ eV}$ , assuming

it to be in  $^{28}\text{Si}$ . If it is a p-wave resonance in  $^{29}\text{Si}$ , then  $g\Gamma_\gamma\Gamma_n/\Gamma = 1.0\text{ eV}$ . The latter value for the radiative width would be more usual for this mass region.

$$^{40}\text{Ar} + n, E_n = (58 \pm 4)\text{keV} (J_c^\pi = 5/2^+, l_n = 2)$$

Transitions are observed to the  $7/2^-$  ground state in  $^{40}\text{Ar}$  at  $E_n = (58 \pm 4)\text{keV}$ . This is seen clearly in Fig. 5 along with transitions to the  $5/2^-$  first excited state. Assuming dipole transitions, the resonance is d wave with  $J_c^\pi = 5/2^+$ .

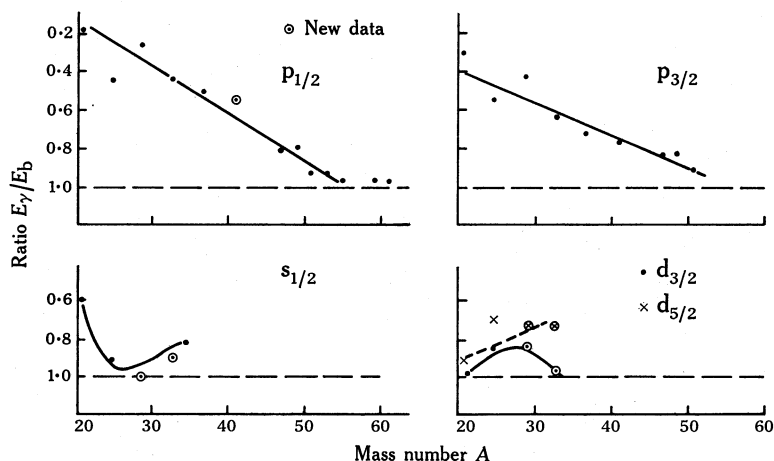


Fig. 6. Plots of the ratio of the  $\gamma$ -ray energy  $E_\gamma$  to the neutron binding energy  $E_b$  against mass number  $A$  for the strongest transition to each final state assignment for even-even target nuclei.

### Radiation Widths

Bergqvist *et al.* (1967) obtained average radiation widths of  $1.4 \times 10^{-3}$  W.u. for E1 and  $20 \times 10^{-3}$  W.u. for M1 (based largely on aluminium data) for 2s-1d shell nuclei. They concluded that the M1/E1 ratio was small ( $\sim 10^{-2}$ ) for even- $Z$  nuclei and much larger ( $\gtrsim 10^{-1}$ ) for odd- $Z$  nuclei. In the present work we have used a larger  $\Gamma_\gamma$  for the 35 keV resonance in aluminium and on the basis of recent negative parity assignments have shown that strong M1 transitions also occur in fluorine. Our average M1 value is thus larger than that of Bergqvist *et al.* while our E1 average is in good agreement, bearing in mind that different transitions are involved. The M1/E1 ratio is found to be  $\sim 1$  for odd- $Z$  nuclei and  $\sim 10^{-2}$  for even- $Z$  nuclei.

### Strong Transitions

In most decay schemes, irrespective of the resonance  $l$ -value, a few transitions account for about three-quarters of the observed intensities. Thermal spectra also show a small number of strong lines. It was pointed out by Bird (1969) that neutron capture by even-even medium weight nuclei is generally followed by strong transitions to predictable final states. The data then available for negative parity states ( $p_{1/2}$ ,  $p_{3/2}$ ) included fairly extensive thermal capture results in the region  $A = 20$ -90. For the  $s_{1/2}$  positive parity states, however, the data were restricted to the results of Bergqvist *et al.* (1967) for 2s-1d shell keV capture. From the present work it has been possible to use the silicon, sulphur and argon data to supplement previous data.

Fig. 6 shows a set of plots for five shell model states including  $d_{3/2}$  and  $d_{5/2}$ . All transitions are E1. The argon data fit smoothly on the  $p_{1/2}$  curve and a clear minimum is obtained for the  $s_{1/2}$  curve. This is possibly true for the  $d_{3/2}$  and  $d_{5/2}$  states also, although insufficient data from p-wave resonances are available to confirm this. The  $d_{3/2}$  state in  $^{21}\text{Ne}$  appears to be lower than might be expected.

It was argued by Bird (1969) that the shape of the  $p_{1/2}$  and  $p_{3/2}$  plots could be taken as evidence that the neutron capture process is semi-direct. The incoming neutron forms a resonant state which may decay by a transition involving the pairing of this neutron and a core neutron, the pair going into vacant high spin states leaving a low spin hole. The conclusion is then that neutron capture in even-even medium weight nuclei is predominantly a one- or two-stage process, at least for low angular momenta.

The odd-Z nuclei show much less evidence for systematic trends. Where initial and final state configurations are known, all transitions are consistent with the dipole hypothesis. By supplementing the data from this experiment with the sodium and additional aluminium data from Bergqvist *et al.* (1967) and Lundberg and Bergqvist (1970), it is found that there are no systematic changes between thermal and keV capture whether it be s wave or p wave. The picture is confused by the lack of information on spin and parity assignments in sodium, and the recent assignments given to low lying levels in  $^{20}\text{F}$  which differ from previous values.

## Conclusions

The high resolution Ge(Li) spectrometer enables individual resonances to be studied and decay schemes to be established. Where  $l$  values for individual resonances are known from previous work, the dominant decay modes are seen to be dipole transitions. For the even-Z nuclei there is a strong preference for electric rather than magnetic dipole, but for the odd-Z nuclei strong magnetic dipole transitions are observed. The 67.7 keV resonance in silicon has been assigned  $l_n = 1$ . For argon, where no previous data are available, a resonance has been observed at 58 keV and assigned  $l_n = 2$ . In the case of the 67.7 keV resonance in  $^{28}\text{Si}$ , the relatively strong transition to the 2028 keV  $5/2^+$  state enables a  $J^\pi$  allocation of  $3/2^-$  to be made. A resonance has been observed in  $^{29}\text{Si} + n$ , and this is presumed to be the 31.7 keV resonance observed in natural silicon by Allen and Macklin (1973). In the even-Z nuclei, thermal capture shows only very weak transitions to positive parity states whereas, in keV capture, numerous strong transitions are seen to these states. It is clear therefore that p-wave resonances are significant in the present mass region. This behaviour is consistent with the shell model, and previous work (Kenny 1971; Bird *et al.* 1972) has shown similar consistency in the mass regions  $A = 40$ –70 and 90–130. Radiation widths for E1 transitions show typical average values, while M1 transitions in fluorine and aluminium are strong.

## Acknowledgments

The authors acknowledge valuable discussions with Dr J. R. Bird and assistance from Dr D. Chan and the accelerator technical staff. Branching ratio information for the  $^{26}\text{Mg}(p, \gamma)^{27}\text{Al}$  reaction was provided by Dr S. G. Boydell of Melbourne University.

## References

- Allen, B. J., and Macklin, R. L. (1973). Proc. Int. Conf. on Photonuclear Reactions and Applications, March 1973, p. 291.
- Bartholomew, G. A., *et al.* (1967). *Nucl. Data A* **3**, 434.
- Bergqvist, I., Biggerstaff, J. A., Gibbons, J. H., and Good, W. M. (1967). *Phys. Rev.* **158**, 1049.
- Bird, J. R. (1969). Proc. Int. Conf. on Properties of Nuclear States, Montreal, p. 782.
- Bird, J. R., Allen, B. J., and Kenny, M. J. (1969). AAEC Rep. No. TM511; Proc. IAEA Symp. on Neutron Capture Gamma Ray Spectroscopy, Studsvik, p. 587.
- Bird, J. R., Biggerstaff, J. A., Gibbons, J. H., and Good, W. M. (1965). *Phys. Rev. B* **138**, 20.
- Bird, J. R., Kenny, M. J., and Allen, B. J. (1968). *Phys. Lett. B* **27**, 638.
- Bird, J. R., Pattenden, N. J., and Kenny, M. J. (1972). Proc. IAEA Conf. on Nuclear Structure Study with Neutrons, Budapest, p. 460.
- Forster, J. S., Ball, G. C., Davies, W. G., Leslie, J. R., McLatchie, W. T., and Millington, G. F. (1973). *Bull. Amer. Phys. Soc.* **18**, 678.
- Fubini, A., Napoli, A., Prosperi, D., and Terrasi, F. (1970). CNEA Rep. No. RT/F1(70)47.
- Gove, N. B., and Wapstra, A. H. (1972). *Nucl. Data A* **11**, 2, 3.
- Hardell, R., and Hasselgren, A. (1969). *Nucl. Phys. A* **123**, 215.
- Hardell, R., Idetjarn, S. O., and Ahlgren, H. (1969). *Nucl. Phys. A* **126**, 392.
- Johnston, I. P., Castel, B., and Sostegno, P. (1971). *Phys. Lett. B* **34**, 34.
- Kenny, M. J. (1971). *Aust. J. Phys.* **24**, 805.
- Longo, D. S., Lawson, J. C., Alexander, L. A., Hichwa, B. P., and Chagnon, P. R. (1973). *Phys. Rev. C* **8**, 1347.
- Lundberg, B., and Bergqvist, I. (1970). *Phys. Scr.* **2**, 256; Proc. IAEA Symp. on Neutron Capture Gamma Ray Spectroscopy, Studsvik, p. 667.
- Macklin, R. L., and Winters, R. R. (1973). *Phys. Rev. C* **7**, 1766.
- Nystrom, G., Lundberg, B., and Bergqvist, I. (1970). RIND Rep. No. FOA C440-22.
- Pronko, J. G. (1973). *Phys. Rev. C* **7**, 127.
- Rasmussen, N. C., Orphan, V. J., Harper, T. L., Cunningham, J., and Ali, S. A. (1970). Gulf Atomic Rep. No. GA-10248.
- Singh, U. N., *et al.* (1971). Proc. Int. Conf. on Statistical Properties of Nuclei, Albany, p. 81 (Plenum: New York).
- Skorka, S. J., Hertel, J., and Retzschmidt, T. W. (1966). *Nucl. Data A* **2**, 4, 349.
- Spilling, P., Gruppelaar, H., De Vries, H. F., and Spits, A. M. J. (1968). *Nucl. Phys. A* **113**, 395.
- Spits, A. M. J., Op der Kamp, A. M. K., and Gruppelaar, H. (1970). *Nucl. Phys. A* **145**, 449.

